

was varied from 4 to 20. The inverse of  $[f]$  was evaluated numerically. The calculations were performed using a digital computer employing twelve digit accuracy for a number of  $EI_1$ ,  $EI_2$ ,  $L$ , and  $\alpha_0$  combinations. Loadings  $S_5$  and  $S_8$  were applied independently, and deflections  $u_5 - u_8$  calculated in each instance. Solution by the formulations of Eqs. (7) and (9) gave identical results as expected. The % error between the segmentally twisted beam deflections and those calculated by the continuous twist formulation of Eqs. (7) and (9) is given in Fig. 2 for a few of the cases considered.

The range of parameters considered is felt to be of practical interest, and based upon the cases considered, it is evident that the errors due to segmental twist modeling are most significant for the coupling deflections and for bending which is predominantly in the stiffer plane. Also it is noted that these errors are strongly dependent upon the total twist and only little influenced by  $EI_1/EI_2$  variations. For the several total beam lengths employed, the % error was found to be independent of this parameter. In all cases considered however, the error produced by the segmental approximation is less than 1% if the number of piecewise twisted elements employed is ten or greater.

### References

<sup>1</sup> Houbolt, John C. and Brooks, George W., "Differential Equations of Motion for Combined Flapwise Bending, Chordwise Bending, and Torsion of Twisted Nonuniform Rotor Blades," TN 1346, 1958, NACA.

<sup>2</sup> Carnegie, William, "Static Bending of Pre-Twisted Cantilever Blading," *Proceedings of the Institution of Mechanical Engineers*, Vol. 171, 1957, pp. 873-894.

<sup>3</sup> Przemieniecki, J. S., *Theory of Matrix Structural Analysis*, McGraw-Hill, New York, 1968, pp. 148-150.

## Flutter of Low Aspect Ratio Plates

E. H. DOWELL\* AND C. S. VENTRES†  
Princeton University, Princeton, N.J.

SPRIGGS, Messiter, and Anderson<sup>1</sup> have recently presented an interesting and valuable explanation of the flutter behavior of a (two-dimensional) plate under in-plane tension load in the limit as the tension stiffness dominates the bending stiffness, i.e., a membrane. They develop an asymptotic analysis based on the hypothesis of a boundary layer at the plate edge and the presence of two length scales. The insight into this boundary-layer behavior was obtained by examining the natural modes of a pure membrane under aerodynamic loading, although there is more than a hint of such behavior in Dugundji's results<sup>2</sup> for plates with finite bending stiffness.

It is the purpose of the present Note to point out that the interpretation of the results of Spriggs et al. may be generalized to include three-dimensional plates and thus also explain the failure of infinitely long traveling wave analyses for low aspect ratio plates at high supersonic speeds and, implicitly, the success of such analyses at subsonic Mach numbers.<sup>3-5</sup>

The mathematical model studied by Spriggs, Messiter, and Anderson was a two-dimensional plate under tension using linear plate theory and piston theory aerodynamics.

Received December 11, 1969; revision received February 13, 1970. This work was supported by NASA Grant NGR 31-001-059.

\* Associate Professor, Department of Aerospace and Mechanical Sciences. Member AIAA.

† Research Associate, Department of Aerospace and Mechanical Sciences.

The equation of motion for such a physical system is (here we use essentially the notation of Dugundji<sup>2,4</sup> and Dowell<sup>5</sup>)

$$D \frac{\partial^4 w}{\partial x^4} - N_x \frac{\partial^2 w}{\partial x^2} + \frac{\rho U^2}{M} \frac{\partial w}{\partial x} + \frac{\rho U}{M} \frac{\partial w}{\partial t} + \rho_m h \frac{\partial^2 w}{\partial t^2} = 0 \quad (1)$$

These equations can be nondimensionalized as

$$\epsilon^2 \frac{\partial^4 w}{\partial \xi^4} - \frac{\partial^2 w}{\partial \xi^2} + \epsilon^2 \lambda \frac{\partial w}{\partial \xi} + \left( \frac{\lambda \mu}{M} \right)^{1/2} \epsilon^2 \frac{\partial w}{\partial \tau} + \epsilon^2 \frac{\partial^2 w}{\partial \tau^2} = 0 \quad (2)$$

where

$$\epsilon^2 \equiv D/a^2 N_x, \lambda \equiv \rho U^2 a^3 / DM, \mu \equiv \rho a / \rho_m h \\ \tau \equiv t(D/\rho_m h a^4)^{1/2}, \xi \equiv x/a$$

Assuming

$$w(\xi, \tau) = \bar{w}(\xi) e^{ik\tau}$$

the eigenvalue problem becomes

$$\epsilon^2 d^4 \bar{w} / d\xi^4 - (d^2 \bar{w} / d\xi^2) + \epsilon^2 \lambda (d\bar{w} / d\xi) + \epsilon^2 B \bar{w} = 0 \quad (3)$$

where

$$B \equiv [(\lambda \mu / M)^{1/2} iK - K^2]$$

Spriggs et al. introduced the following variables:  $\alpha^2 \equiv \lambda \epsilon^2$  and  $\gamma \equiv (\lambda \mu / M)^{1/2} \epsilon^2$  and obtained stability boundaries (where the imaginary part of the eigenvalue  $K$  becomes negative) in terms of  $\alpha$ ,  $\gamma$ , and  $\epsilon$ . The specific mathematical techniques used lead to asymptotic expansions in  $\epsilon$ , for small  $\epsilon$ , allowing for two length scales, one of order 1 and one of order  $\epsilon$ .

Now let us consider a more general problem, that of a three-dimensional plate under tension loads in two directions. (Actually, what follows could be generalized to include structural damping, an elastic foundation and orthotropicity, see for example Dugundji<sup>2</sup> as well as earlier work by Hedgepeth<sup>6</sup> and Houbolt.<sup>7</sup>) Thus,

$$D \left[ \frac{\partial^4 w}{\partial x^4} + 2 \frac{\partial^4 w}{\partial x^2 \partial y^2} + \frac{\partial^4 w}{\partial y^4} \right] - N_x \frac{\partial^2 w}{\partial x^2} - N_y \frac{\partial^2 w}{\partial y^2} + \frac{\rho U^2}{M} \frac{\partial w}{\partial x} + \frac{\rho U}{M} \frac{\partial w}{\partial t} + \rho_m h \frac{\partial^2 w}{\partial t^2} = 0 \quad (4)$$

Nondimensionalizing,

$$\frac{\partial^4 w}{\partial \xi^4} + 2 \frac{\partial^4 w}{\partial \xi^2 \partial \eta^2} \left( \frac{a}{b} \right)^2 + \frac{\partial^4 w}{\partial \eta^4} \left( \frac{a}{b} \right)^4 - R_x \frac{\partial^2 w}{\partial \xi^2} - R_y \frac{\partial^2 w}{\partial \eta^2} \left( \frac{a}{b} \right)^2 + \lambda \frac{\partial w}{\partial \xi} + \left( \frac{\lambda \mu}{M} \right)^{1/2} \frac{\partial w}{\partial \tau} + \frac{\partial^2 w}{\partial \tau^2} = 0$$

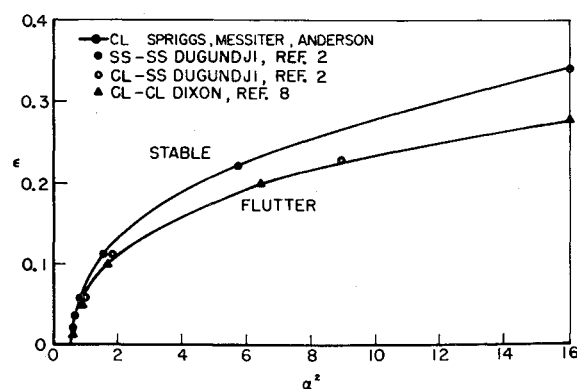


Fig. 1 Width/length ratio vs flutter dynamic pressure.

where

$$\xi \equiv x/a, \eta \equiv y/b, R_x \equiv N_x a^2/D, R_y \equiv N_y a^2/D \quad (5)$$

Using a one-mode approximation in the  $y$  variable

$$w(\xi, \eta, \tau) = g(\eta) \bar{w}(\xi) e^{ik\tau}$$

and applying Galerkin's method we have

$$\epsilon^2 (d^4 \bar{w}/d\xi^4) - (d^2 \bar{w}/d\xi^2) + \lambda \epsilon^2 (d\bar{w}/d\xi) + \epsilon^2 B \bar{w} = 0$$

where

$$\begin{aligned} \epsilon^2 &\equiv C_1/[R_x C_1 + 2(a/b)^2 C_2] \\ B &\equiv [(C_4/C_1)(a/b)^4 + R_y(a/b)^2 C_2/C_1 + \\ &\quad (\lambda \mu/M)^{1/2} i K - K^2] \quad (6) \end{aligned}$$

$$C_1 \equiv \int_0^1 g^2 d\eta, C_2 \equiv - \int_0^1 \frac{d^2 g}{d\eta^2} g d\eta$$

$$C_4 \equiv \int_0^1 \frac{d^4 g}{d\eta^4} g d\eta$$

Note  $C_1, C_2, C_4 > 0$ . Clearly there is a perfect analogy between Eqs. (3) and (6). This result is not new, of course, having been noted by the authors of Refs. 2, 6, and 7 among others.

Thus, we may 1) use the boundary-layer concept of Spriggs et al.<sup>1</sup> to interpret earlier studies of three-dimensional plates for large  $a/b$ , i.e., small  $\epsilon$  and 2) use the numerical results of earlier studies by Dugundji<sup>2</sup> and Dixon<sup>8</sup> for large  $a/b$  to improve the quantitative character of the asymptotic stability boundaries established by Spriggs, Messiter, and Anderson.

Let us first consider the second item since it may be disposed of in short order. From Dugundji and Dixon, we have results for  $\mu = R_x = R_y = 0$  and various  $a/b$  that can be used to compare with the results of Ref. 1. (Dugundji also gives extensive results for  $\mu \neq 0, R_x \neq 0, R_y \neq 0$ , etc.) For this special case, in the notation of Spriggs et al.,

$$\begin{aligned} \alpha^2 &\equiv \lambda \epsilon^3 = \lambda \{ [C_1/2C_2(a/b)^2] \}^{3/2}, \gamma \equiv 0 \\ \epsilon &\equiv \{ [C_1/2C_2(a/b)^2] \}^{1/2} \end{aligned}$$

Note that  $\lambda \epsilon^3 \equiv \alpha^2$  is essentially  $\lambda$  nondimensionalized by  $b$  rather than  $a$ , while  $\epsilon \sim b/a$ . Dugundji and Dixon have previously used these variables in plotting their results. In Fig. 1, we compare results of Refs. 1, 2, and 8. Incorporating  $C_1$  and  $C_2$  into the definitions of  $\alpha^2$  and  $\epsilon$  collapses results for various  $y$  boundary conditions and (hence various  $g$ ) into single curves. In addition, we expect results for various  $x$  boundary conditions to collapse to a single point as  $\epsilon \rightarrow 0$ . This is indeed the case as may be seen in Fig. 1. Somewhat surprisingly, the results from Spriggs et al., which were developed for clamped-edge boundary conditions agree better with results of Dugundji for simply-supported edges than those from Dugundji, Dixon for clamped edges. The reason for this quantitative difference is not known. Presumably the numerical results of Dugundji, Dixon are more accurate. It should be noted that Dugundji's clamped results are for a plate clamped on leading and trailing edges and simply supported on the side edges, whereas Dixon's results are for a plate clamped all around. By the previous scaling, these results fall on a single curve.

Interesting as the previous comparisons are, the more interesting aspect is the understanding which the boundary-layer concept of Spriggs et al. brings to other "paradoxes" in the panel flutter literature. In particular, the limitations of an infinitely long, traveling wave analysis<sup>3-5</sup> for plates of large  $a/b$  are now clear. In such an analysis, plate deformations are assumed to be constant amplitude traveling waves with wavelength comparable to the plate width. On the other hand, the analysis of Spriggs et al., as interpreted here, clearly shows that the plate deformation is one in which the length scale of the traveling wave changes from one com-

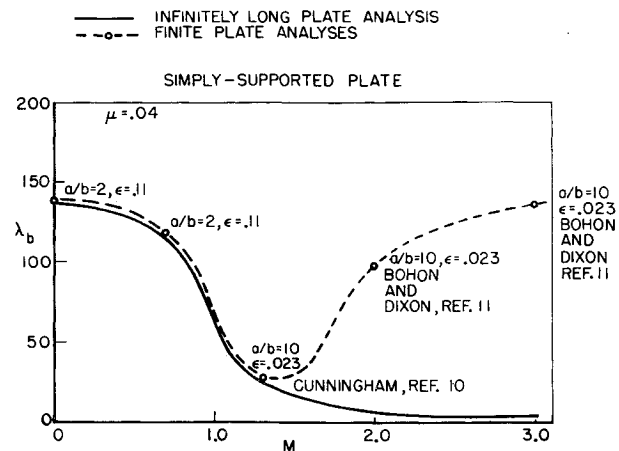


Fig. 2 Flutter dynamic pressure vs Mach number.

parable to plate length to one comparable to plate width as the plate is traversed from leading to trailing edge. In addition, there is a rapid exponential modulation of the plate deformation with length scale on the order of plate width as one approaches the trailing edge.

Hence, the traveling wave analysis is inadequate at high supersonic Mach number. However, at subsonic Mach number the plate deformation is essentially one of constant amplitude with wavelength comparable to the plate width based on the finite length experimental and theoretical results of Dugundji<sup>4</sup> et al. for a plate on an elastic foundation as well as previously unpublished results by Ventres and Dowell using the analysis of Ref. 9 for low-aspect ratio plates. These results show no significant exponential spatial growth near the trailing edge. In Fig. 2, we compare results over a range of Mach number as obtained by analyses using the full linearized aerodynamic theory, 1) with the finite length accounted for and 2) from the infinitely long plate, traveling wave analysis. Simply-supported edge conditions apply. The results of type 1 at  $M = 1.3, 2.0$  and  $3.0$  were obtained from Cunningham's flutter analysis by Cunningham,<sup>10</sup> Bohon and Dixon.<sup>11</sup> The other results are derived from the present authors. The good agreement at  $M = 1.3$  is probably to some extent fortuitous since there is some significant exponential spatial growth in the flutter mode; however, it is less than at  $M = 3$ . Note that good agreement at  $M = 0.7$  is obtained at  $a/b = 2$  indicating the asymptote,  $a/b \rightarrow \infty$ , is reached more rapidly at subsonic Mach numbers than supersonic ones. Ventres has shown in unpublished results for clamped edges that at  $M = 0$  the results for  $a/b = 2$  and 4 agree very closely providing further support for this conclusion.

### Conclusions

The asymptotic analysis of Spriggs, Messiter, and Anderson for a two-dimensional plate under tension can be reinterpreted and used to investigate a wider class of problems. In particular, the limit of large length/width ratio (or low-aspect ratio) plates may be studied and their analysis thus interpreted goes far to explain the previously observed inadequacies of the infinitely long traveling wave model at high supersonic speeds. It also implicitly explains why such a model works at subsonic speeds. In addition, such a reinterpretation of their numerical results allows a wide range of comparison with available data from more conventional analyses by Dugundji and Dixon. There is general agreement, although some discrepancy is noted in terms of quantitative accuracy.

### References

- 1 Spriggs, J. H., Messiter, A. F., and Anderson, W. J., "Membrane Flutter Paradox—An Explanation by Singular Perturba-

tion Methods," *AIAA Journal*, Vol. 7, No. 9, Sept. 1969, pp. 1704-1709.

<sup>2</sup> Dugundji, J., "Theoretical Considerations of Panel Flutter at High Supersonic Mach Numbers," *AIAA Journal*, Vol. 4, No. 7, July 1966, pp. 1257-1266.

<sup>3</sup> Miles, J. W., "On the Aerodynamic Stability of Thin Panels," *Journal of Aeronautical Sciences*, Vol. 23, No. 8, Aug. 1956, pp. 771-780.

<sup>4</sup> Dugundji, J., Dowell, E., and Perkin, B., "Subsonic Flutter of Panels on Continuous Elastic Foundations," *AIAA Journal*, Vol. 1, No. 5, May 1963, pp. 1146-1154.

<sup>5</sup> Dowell, E. H., "Flutter of Infinitely Long Plates and Shells. Part I: Plate," *AIAA Journal*, Vol. 4, No. 8, Aug. 1966, pp. 1370-1377.

<sup>6</sup> Hedgepeth, J. M., "Flutter of Rectangular Simply Supported Panels at High Supersonic Speeds," *Journal of Aeronautical Sciences*, Vol. 24, No. 8, Aug. 1957, pp. 563-573.

<sup>7</sup> Houbolt, J. C., "A Study of Several Aerothermoelastic Problems of Aircraft Structures," *Mitteilungen Aus Institut für Flugzeugstatik und Leichtbau*, Nr. 5, Verlag Leeman, Zurich, 1958.

<sup>8</sup> Dixon, S. C., "Comparison of Panel Flutter Results From Approximate Aerodynamic Theory with Results from Exact Inviscid Theory and Experiment," TN D-3649, 1966, NASA.

<sup>9</sup> Dowell, E. H., "Nonlinear Oscillations of a Fluttering Plate, II," *AIAA Journal*, Vol. 5, No. 10, Oct. 1967, pp. 1856-1862.

<sup>10</sup> Cunningham, H. J., "Analysis of the Flutter of Flat Rectangular Panels on the Basis of Exact Three-Dimensional, Linearized Supersonic Potential Flow," *AIAA Journal*, Vol. 1, No. 8, Aug. 1963, pp. 1795-1801.

<sup>11</sup> Bohon, H. L. and Dixon, S. C., "Some Recent Developments in Flutter of Flat Panels," *Journal of Aircraft*, Vol. 1, No. 5, Sept.-Oct. 1964, pp. 280-288.

## Imperfect Gas Effect in Real Hydrogen Drives

WILLIAM L. GROSE\* AND JOHN E. NEALY\*  
NASA Langley Research Center, Hampton, Va.

### Nomenclature

- $a$  =  $(\partial p / \partial \rho)^{1/2}$  = sound speed  
 $f$  = empirical constant for a given entropy  
 $k$  = empirical constant for a given entropy  
 $M_s$  = shock Mach number  
 $p$  = pressure  
 $s$  = entropy  
 $T$  = temperature  
 $u$  = velocity  
 $v$  = specific volume  
 $z$  = compressibility  
 $\beta$  = empirical constant for a given entropy  
 $\rho$  = density

### Subscripts

- $f$  = final state  
 $i$  = initial state  
 $0$  = reference ( $p_0 = 1$  atm;  $\rho_0 = 1$  amagat)  
 $1$  = state of quiescent test gas  
 $4$  = state of initial driver gas

**I**MPULSE facilities (e.g., the shock tunnel) have been extensively used for the production of high-enthalpy flows in various gas mixtures. The use of statically heated hydrogen as a driver has become quite common.<sup>1,2,3</sup> For the upper performance limits, the hydrogen might be compressed to

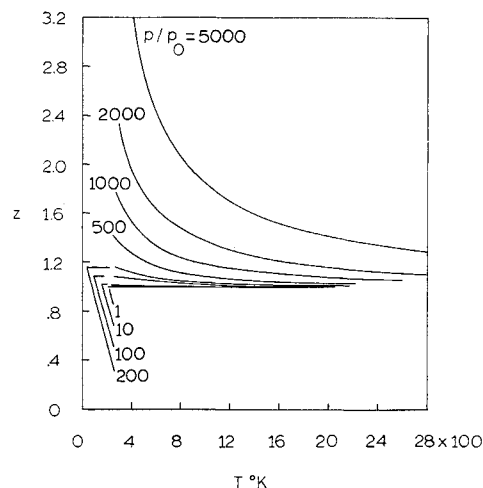


Fig. 1 Compressibility factor for hydrogen.

pressures as high as 2000 atm at 800°K. For these conditions, the assumption of an ideal gas is inadequate due to the existence of large intermolecular forces.<sup>4</sup> Huber<sup>5</sup> has calculated performance of a shock tube using unheated hydrogen drivers at pressures up to 125 atm. The development of an expansion tunnel at LRC required more extensive real hydrogen driver performance calculations. These calculations utilized the equations for thermodynamic properties from Ref. 4. Although this data lacks experimental verification above 600°K, it does continue the trend of the most reliably established properties of hydrogen.<sup>6</sup>

The effects of considering the intermolecular forces can be seen in Fig. 1 which presents  $z$  as a function of  $T$  for pressures of 1-5000 atm. For the typical driver conditions cited, a value of  $z = 1.5$  is attained. Figure 2 is a plot of  $p$  as a function of  $T$  along isentropes. The differential equation governing an isentropic one-dimensional unsteady expansion can be written<sup>7</sup>

$$du = - (dp/\rho a)_s \quad (1)$$

Equation (1) can be readily integrated using the semiempirical entropic equation of Ref. 4

$$p^{(\beta-2)/\beta} (v-f) = k \quad (2)$$

resulting in the following expression

$$\Delta u = [k\beta(\beta-2)]^{1/2} p^{1/\beta} \quad (3)$$

where  $\Delta u$  is the velocity increment imparted to the flow as it expands from an initial pressure to  $p = 0$ . Figure 3 presents values of  $\Delta u$  as a function of  $p$  at constant entropy. With a

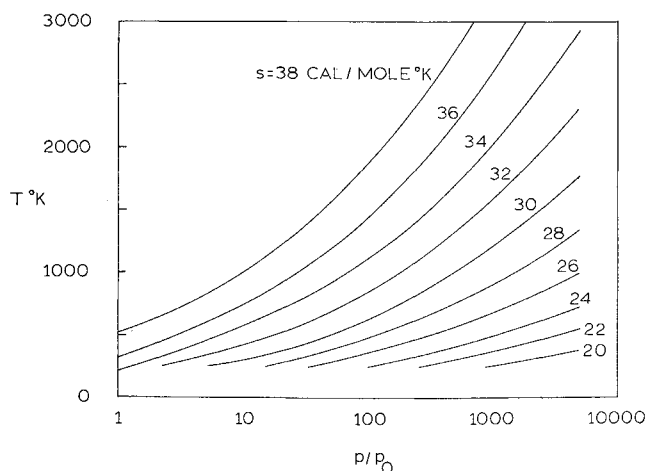


Fig. 2 Pressure-temperature diagram for hydrogen.

Received December 29, 1969; revision received February 20, 1970.

\* Aerospace Engineer, Gas Physics Section, Aero-Physics Division.